Article PDF Available

Imaging human spontaneous photon emission: historic development, recent data, and perspectives

January 2013
January 2013 · 15:27

Authors:

Eduard van Wijk
Leiden University

Abstract and Figures

Imaging of spatial distributions of ultra-weak spontaneous photon emission (UPE) in living systems started in the mid 1980's in Japan. This chapter begins with a historic overview on the progression in sensitivity of the imaging technology allowing not only plants but also animal and human body parts to be imaged. Imaging was initially performed in small light-tight chambers using 2-dimensional photomultiplier tube systems. More recently, with the help of a charge-coupled device (CCD), larger body surface were imaged at some distance. A few recent examples on human body emission demonstrate specific emission patterns and suggest dynamic fluctuations within the pattern. Data further suggest slow fluctuations in emissions. The dynamic spatial UPE patterns allow to formulate novel hypotheses to research the biological energy systems underlying this fascinating light phenomenon and to evaluate the possibilities for a diagnostic perspective.


Ultra-weak photon emissio…


A series of the ultra-weak phot…

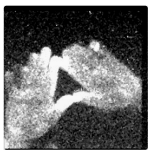
A series of images of the…


A series of ultra-weak photon…


Illustrative examples of…

Trends in Photochemistry & Photobiology
Vol. 15, 2013

Review

Imaging human spontaneous photon emission: Historic development, recent data and perspectives

Wijk[1,3], Eduard P. A. Van Wijk[1,2,3], Yan Schroen[1] and Jan van der Greef[1,2,4]
[1]Sino-Dutch Centre for Preventive and Personalized Medicine, [2]Division of Analytical Biosciences, LACDR, Leiden University, Leiden, [3]Meluna Research, Amersfoort,
[4]TNO Netherlands Organization for Applied Scientific Research, Zeist, The Netherlands

ABSTRACT

Imaging of spatial distributions of ultra-weak spontaneous photon emission (UPE) in living systems started in the mid 1980's in Japan. This chapter begins with a historic overview on the progression in sensitivity of the imaging technology allowing not only plants but also animal and human body parts to be imaged. Imaging was initially performed in small light-tight chambers using 2-dimensional photomultiplier tube systems. More recently, with the help of a charge-coupled device (CCD), larger body surface were imaged at some distance. A few recent examples on human body emission demonstrate specific emission patterns and suggest dynamic fluctuations within the pattern. Data further suggest slow fluctuations in emissions. The dynamic spatial UPE patterns allow to formulate novel hypotheses to research the biological energy systems underlying this fascinating light phenomenon and to evaluate the possibilities for a diagnostic perspective.

KEYWORDS: ultra-weak photon emission (UPE), charge-coupled device (CCD), imaging, human body, anatomical distribution

INTRODUCTORY OVERVIEW

Ultra-weak photon emission (UPE) of the human body has been studied since 1979 [1]. Its detection was possible using highly sensitive photomultiplier tubes. The interest in imaging such emission increased in the mid-1980's. The knowledge of such imaging began spreading with the 1984 publication by Tsuchiya, Inuzuka, Kurono and Hosoda of Hamamatsu Photonics Inc. regarding a Photon-counting Image Acquisition System (PIAS) employing a position sensitive detector in conjunction with a microchannel plate [2]. The imaging photomultiplier tube consisted of a photocathode, microchannel plates to provide gain and a position sensitive detector. The wavelength range of the detector was from 350 nm to 850 nm.

A special project for two dimensional photomultiplier counting techniques was initiated as part of the "Inaba Biophoton Project" in Japan in 1986. The project was funded by the Exploratory Research for Advanced Technology (ERATO), a subsidiary of the Research Development Corporation of Japan (later, Japan Science and Technology Corporation). Spatial distribution of ultra-weak light emission by living organisms offers information about such emission within a specimen.

This system was developed and first used by Inaba and coworkers for the two-dimensional detection of ultra-weak photon emission of soybean seeds and roots as described in different publications [3-7]. The images of germinating soybeans were obtained after keeping the specimen in complete darkness in stable conditions for 5 days in order to eliminate the possible effects of delayed luminescence. Although the average count rate

*Corresponding author:
epa.vanwijk@lacdr.leidenuniv.nl

(12 counts/sec) of ultra-weak photon emission was relatively low, remarkable emission was observed in the segment of hypocotyl, the junctional region between radicle and plumule. It was concluded that the emission is strongest in areas where active cell division is taking place for growth.

The two-dimensional photon imaging and counting system of Hamamatsu Photonics was subsequently utilized to clarify the emission of the seedling as a result of physical injury. Suzuki the injury (when the wound had completely healed), the image no longer revealed any clear pattern. UPE intensity returned to normal levels after the scab had fallen off.

In Inaba's laboratory, a special research line was developed utilizing two dimensional photo multiplier counting techniques to make images of human UPE [11-14]. The sensitivity of the system also made it possible to image light emission from a human body surface when the body parts were placed close to the camera system (as is the case

image of light from injured soybean seedlings revealed a 7-20 times higher intensity centred around the injury. The emission intensity was also higher at the root system (hypocotyl and the radicle) away from the site of the injury. The simultaneous increase of light emission at the root system far away from the injury site was very interesting and offered clues to the transfer of information within the living system.

The same research team [9] also used intact and injured soybean seedlings to show that the emission intensity increases rapidly on the cotyledon as soon as H_2O_2 was applied. However, the emission intensity of the injured seedling was far stronger in the central part of the cotyledon (including the intersection point of the cut) than in the peripheral region, in contrast with the intact controls. The authors noted that responsive emission also took place in the root system distant from the injury.

Inaba and colleagues [9, 10] additionally reported that a weak light emission from injured animals could be imaged. They placed a lesion on the back of the animals in the form of a circle 10 mm in diameter. The UPE intensity increased on this injury. The image obtained immediately after creating the lesion did not show any clear pattern or localization. The image was more clear 48 hours after the injury, resembling the shape of the wound, whereas the emission intensity continuously rose. The emission intensity was at the maximum between the third and the fifth day after injury. From the sixth day of the injury the emission intensity began to decrease. On the eighth day of

the index and middle fingers and the lowest intensity in the middle of the palm region. Inaba's team studied the light emission from the fingers in relationship to the metabolic disease of hypothyroidism (a lower state of metabolic activity). In 1994, Inaba's team demonstrated that they could use the measurements from the middle and index fingers of the left hand to differentiate hypothyroidism from control subjects [11]. They reported that the UPE intensity of patients with hypothyroidism was always lower than that of the controls. Lower emission intensity was also observed in the case of patients whose thyroids glands had been removed.

The researchers also compared the UPE from the back of the left and right index fingers. It was observed that the emission intensity was higher at the right index finger and the distribution of the emission intensity was also different for the two fingers. Although the reason for such a difference was not clear, they speculated that it could be attributed to individual differences or the right handedness of the subject or the differences in activity of the acupuncture points [12]. The UPE could also be measured at other regions of the human body surface. The researchers, however, limited their choice to human hands with a view of developing a simple and easy non-invasive technique for diagnostic purposes in the future [13, 14].

In the mid 1990's, the video intensified measuring system of Hamamatsu Photonics was modified in Inaba's laboratories. The ultra-weak photons emitted from the specimen were imaged onto the

detector assembly by a lens with a focal length and aperture of infinity and 0.82, respectively. The detector assembly consisted of a sensitive photocathode and a microchannel plate. The active surface of the photocathode was 15 mm in diameter and the surface under investigation was approximately 1 cm^2. The projected photon image on the photocathode generated photoelectrons which were multiplied by the microchannel plate and then focussed on the imaging tube. The two-dimensional positions of the incident ultra-weak photons were computed by an image processor and displayed on a monitor in a 512 x 512 pixel (picture element) format. Improved equipment

to characterize the dynamics of UPE in the single photoelectron counting region, was then used to explore the relationship between a physiological state and UPE phenomena.

The new technology was first used with soybean seedlings as a model to observe the UPE response under various conditions of physical or chemical stimulation [16]. The UPE image from a soybean seedling and its time course was determined at five different areas. The kinetics of the emission intensity was characteristically different for each area, with the appearance of two peaks at different time intervals during the first 20 h of the measurements. The improved analysis clearly

cells was implanted into the left feet of the mice. The photon emission measurement was performed 2 weeks after implantation. At that time, the tumors had reached approximately 250 mm^3 in volume. The mice were anesthetized and photon counting was performed (after dark adaptation) for 2 h per mouse. The data from the left foot tumor and the control (right foot without tumor) were compared. Photon count per unit area was calculated in the tumor as well as in normal regions (after subtraction of the background counts). Ultra-weak photon emission was evident in the implanted tumor region containing actively proliferating cancer cells.

The improvement of UPE imaging technology continued and in 1996 Kobayashi and colleagues published about an even newer technology for two-dimensional space-time characterization and correlation analysis of UPE information [16]. However, the image resolution was restricted by the integration time and the detection limit of photon counting was restricted by the quantum noise of the detection.

The number of photoelectrons that exceed the dark count fluctuations, for a given measurement period and area, actually determines the signal-to-noise ratio for the measurement system. The novel technique to calculate the intensity kinetics at several regions was based on continuous and simultaneous measurement of time series and position data of photoelectron pulses from two-dimensional photon counting tube. This approach, the root tip was also displayed. Emission intensity of the cut region increased and remained at a high level for 3 h. Significant changes in photon emission intensity were observed at a distant position away from the injury site (a manifestation of response to injury that was reported earlier). In this study, a typical result was also documented when a high concentration of H_2O_2 was added to the root tip. A remarkable enhancement of UPE was observed at the hypocotyl region which is distant from the root tip. This photon emission response at different regions, not in direct contact with H_2O_2, was the first observation of this kind for such a condition.

In a 1997 paper [17], Kobayashi and colleagues reported the first UPE images of a germinating seedling that was obtained utilizing a highly sensitive charge-coupled device (CCD) camera. They compared the performance of the CCD camera with conventional low-level light detectors and demonstrated the potential usefulness of the CCD camera for UPE imaging. Although the conventional imaging systems used a two-dimensional photon counting tube that had excellent sensitivity, the quantum efficiency of the photocathode in this system was very low (approximately 20% at peak wavelength of 400 nm and less than 5% in the red or near-IR regions). In the wavelength region above 700 nm, the cooled CCD camera was advantageous over the two-dimensional photon counting tube. They further deduced that if the CCD is operated at an extremely low dark current and for longer times

in order to reduce the contribution of the read-out noise, the signal-to-noise ratio of the CCD camera would be superior to the conventional two-dimensional photon counting tube under similar conditions of wavelength and measurement time.

Meanwhile, Kobayashi and colleagues continued the biological applications of the two-dimensional imaging technology. In 1999, they demonstrated for the first time images of ultra-weak photon emission from a rat's brain [18]. The equipment used in these experiments consisted of a two-dimensional photon counting tube with a photocathode measuring 40 mm in diameter, a highly efficient lens system and an electronic device to record time series of a photoelectron train with spatial information. The sensitivity and over the skull. To clarify the origin of photon emission they inserted a thin plate between the dura mater and parietal bone to shield light from the cortex. However, this region lacked intensity suggesting that the photons emanating from the brain tissue and moving through the skull are the chief contributors to the UPE image. In these studies, the researchers estimated the θ-wave component of the EEG power spectrum. Temporal changes of the photon emission intensity were then compared with that of the θ-wave activity and found to be comparable. They then analyzed the correlation between photon emission and θ-wave activity for animals where the parietal bones were removed and those that have an intact skull. Although emission intensities observed through

flux density of the system was experimentally estimated to be 9.9 x 10^{-17} W/cm^2 with a 1 s observation time. Ultra-weak photon emission was demonstrated from an exposed rat's cortex in vivo without adding any chemical agent or employing external excitation. The researchers compared the image of UPE with one obtained after cardiac arrest. The intensity after cardiac arrest was depressed by approximately 60%. The regional properties of the time courses of emission intensity were also demonstrated indicating the potential usefulness for spatiotemporal characterization of photon emission with mapping of physiological information such as oxidative stress. The technology was further utilized to extract information from central nervous system activity [19]. They reported on the correlation of the emission intensity with the electro-encephalographic activity that was simultaneously measured on the cortical surface. To record EEG activity, silver ball electrodes were inserted into the skull over both hemispheres. In those experiments the researchers produced forebrain ischemia by using a four-vessel occlusion model. The vertebral arteries were occluded bilaterally, followed by bilateral (but reversible) ligation of the common carotid artery. The study led to typical patterns of UPE images of normal brain and flat EEG in case of brain ischemia. The intensity during ischemia was comparable to that of cardiac arrest. These images were observed

between photon emission intensity and the θ-wave component of the EEG power spectra. It was evident that the imaging of ultra-weak photon emission from a brain constitutes a novel method with the potential to extract pathophysiological information associated with neural metabolism and oxidative dysfunction of the neural cortex.

Towards human body imaging

A recent step in human photon emission was the utilization of the CCD camera system in a dark room at the laboratory of Kobayashi [20-24]. A chair was placed inside a dark room and subjects were measured in sitting position after dark adaptation. A cryogenically cooled CCD camera system that incorporates a CCD42-40 NIMO Back Illuminated High Performance CCD Sensor having full-frame architecture (CCD42-40, e2v technologies, UK) was used for the imaging of human ultra-weak photon emission. Operating temperature of the CCD sensor is -100°C, resulting in a dark signal (electronic noise) of 0.65 e^-/pixel/h. Spectral response of the CCD ranges over 400-900 nm with quantum efficiency of >90% at the peak wavelength of 550 nm. The measurement was carried out in binning mode, resulting in the imaging format of 256 x 256 pixels. The magnification of the lens system for imaging torso and arms was approximately 0.03 and the magnification for imaging the face and

hand was approximately 0.13. The sensitivity of the imaging system facilitated the recording of the UPE image from the upper frontal torso, head, neck and upper extremities of a single subject sitting at a distance of 100 cm in front of the CCD camera for a period of 30 min. During body imaging, participant was naked from the waist up. Differences in UPE were present in the ventral and dorsal images both of the torso and upper extremities (Figure 1). As illustrated in the ventral image of the superior part of the body, UPE intensity around the face and neck was highest and gradually decreased over the torso and subsequently the abdomen (Figure 1A). A gradual decrease in intensity from the superior central torso to its lateral dimensions was recorded. Dorsally, the highest intensity was emitted from the neck (Figure 1B). The image of the arm of the same subject illustrated how the low intensity of

In recent studies with the improved CCD camera and lens system, Kobayashi and colleagues [24] decided to investigate the temporal variations of UPE across the day from five healthy males in their 20's. From one week before the experiments, subjects were subjected to normal light-dark conditions and allowed to sleep from 0:00-7:00 A.M. Subjects were not allowed to use cosmetics including aftershave lotion. On the days of photon imaging, volunteers were kept in a room (400 lux of light) adjacent to the dark room. Volunteers had lunch at 12:30 P.M. hours and dinner at 18:30 P.M. The average time of sleep onset was 23:30 hours and that for awakening was 06:15 hours. The subjects were one by one invited to sit in a relaxing chair in the darkroom. For imaging purposes, the body surface was cleaned. Each day of the 3 day project, the subject remained for 15 minutes in the dark room in order

were compared with the UPE recordings of the same subject utilizing a moveable photomultiplier system [22, 23]. The CCD images from the upper frontal torso, head, neck and upper extremities corresponded with the data of multi-site recordings utilizing the moveable photomultiplier system. This anatomical emission pattern using the moveable photomultiplier system was later confirmed in studies with up to 60 human subjects [25, 26].

CCD camera. Measurements were carried out every 3 hours from 10:00 A.M. to 22:00 P.M. Data clearly demonstrated the daily variation of photon emission. The photon emission intensity on the face and upper body appeared to display time-dependent changes. Averaging the daily variation across the 5 volunteers resulted in a general (typical) daily fluctuation pattern. The photon emission was weak in the morning, increased in the afternoon and peaked in the late afternoon.

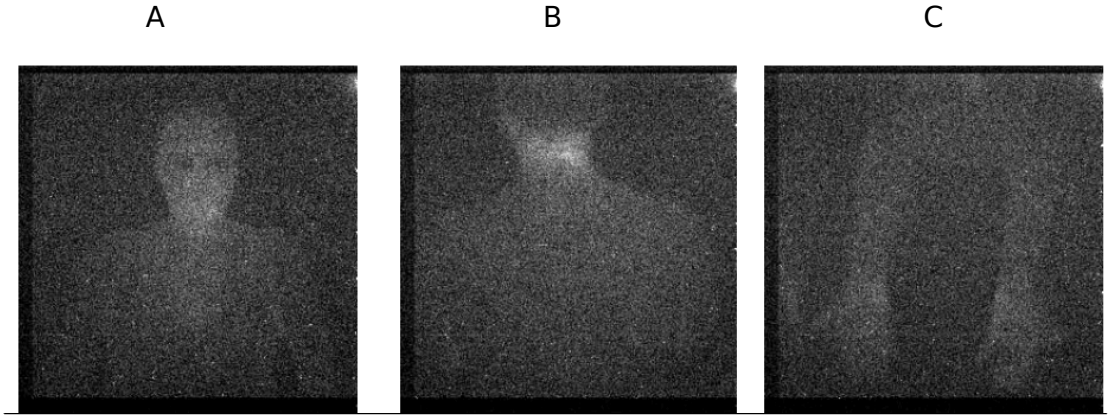

Figure 1. Ultra-weak photon emission of a human subject. The panels represent images of the ventral (**A**) and dorsal (**B**) torso and arms (**C**) of the subject.

It suggested that there is a diurnal rhythm of photon emission from the human body. To further support this conclusion, three volunteers were kept awake and photon emission was measured at 1:00, 4:00 and 7:00 AM. Photon emission formed a peak at late afternoon, then gradually decreased and stayed low between 1:00-7:00 AM. The images showed that emission intensity of specific areas as well as the size of areas with equal brightness could fluctuate. Data indicated that the diurnal rhythm of photon emission was caused by an endogenous circadian mechanism. In this experiment, the surface body and oral temperatures were taken vis-à-vis thermography. The lack of correlation of daily photon intensity and temperature suggested that the diurnal rhythm of photon emission was not a consequence of change in temperature.

The observed daily variation of photon emission from the face and frontal torso and the non-homogeneous distribution of the emissions of these anatomical areas raised several questions

both the left and the right foot at consecutive days.

A discussion of the intensity fluctuations in hands is based on two series of images. The first series includes images of the palms of both hands. Such images are difficult to obtain due to the positioning of the subject. Exposing the hand palms in sitting position to the camera for 20 min is extremely difficult and results in a high degree of uncontrollable movement and subsequent loss of sharpness. Figure 3 images were made with the subject in a lying position with the hands above the head and thumbs and index fingers pointing towards each other. In this position the palms are exposed to the CCD camera in a position which is relatively relaxed. However, a little loss of sharpness cannot be totally avoided. Each image includes the left and right palm. As with the feet, the variability of palm emission intensity was high within a single subject. An interesting aspect is noticed when the images are compared in the

upper body, the hands and feet demonstrated a distinct non-homogeneous distribution of the emission. The typical feature in hand's and foot's emission pattern was that the emission was highest at the tip of the fingers and toes at the areas covered by the nails. In the following paragraph, this emission is illustrated to characterize its variability.

Dynamics

Another series of images made in Kobayashi's laboratory focused on hands and feet of a single male subject. The images were captured throughout two consecutive days. Each experimental day, the subject was imaged twice: early morning and late afternoon. For this series, no special measurement protocol was followed because in this preliminary state of the study, data on the variation in hand and foot emission were not available.

The series of foot images is illustrated in Figure 2. Each image includes the left and right foot. The variability of emission intensity was enormous as observed from the differences between right and left foot on both days. Another difference is evidently seen in the intensity of the toe tips of

order of overall intensity (order: B, A, D, C). In particular, the thumb and index finger suggest that the increase in intensity represents a pattern of preferential emission.

Images of the dorsal left and right hands are presented in Figure 4. Most intensity is observed at the tips of the fingers. However, the high emission is not limited to the nails. In some images, the intensity is seen to extend over a larger area (for instance Figure 4A). For the hand images of the palm (Figure 3) and dorsal (Figure 4) sides it was evident that left-right differences are relatively small.

Further progress in emission dynamics: The focus on dorsal of hands

In another study, the attention was focused on the dorsal side of the hand of another single subject. The CCD camera system that was utilized was an iXon 888^{EM}+ (back-illuminated), highly sensitive electron-multiplying CCD (EMCCD) camera system (Andor Technology Ltd, Belfast, Northern Ireland). The system's specifications were CCD201 (e2v technologies Ltd., Essex, UK), pixel format 1024 x 1024, pixel size 13 μm^2, and 16-bits at 1 MHz readout rate. System read-out noise was $<1e^-$ a 16-bit 1MHz readout rate. Dark current was <<1 electrons/pixel/sec. Spectral

Image A

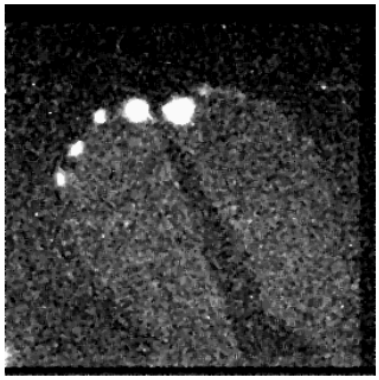

Image B

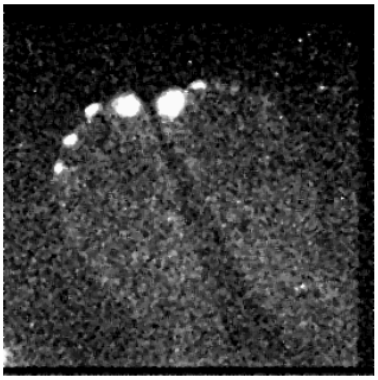

Image C

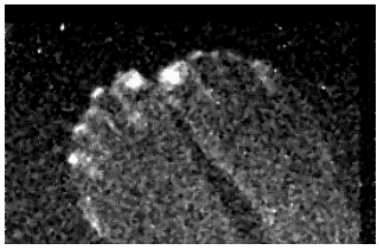

Image D

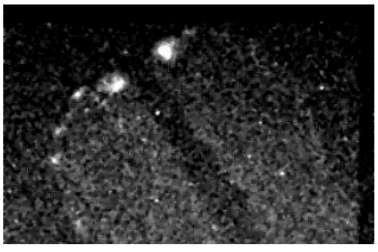

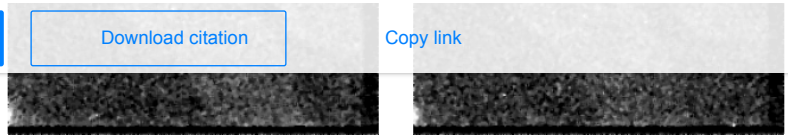

Figure 2. A series of the ultra-weak photon emission images of feet of a single subject. Images were captured throughout two consecutive days. Image A: Day 1, early morning; Image B: Day 1, late afternoon; Image C: Day 2, early morning; Image D: Day 2, late afternoon.

sensitivity of the CCD ranged from approximately 200-1000 nm with a peak (92%) in quantum efficiency at 575 nm. The detector was cooled to -100°C vis-à-vis thermoelectric cooling plus additional cooling was done with a water-cooled chiller (Oasis™ 160LT, Solid State Cooling Systems, NY, USA) set at 15°C to avoid condensation in the camera. When water cooling was utilized, the internal fan could be turned off. Exceptional cooling performance was maintained indefinitely without introducing errors via vibrations from the internal fan. A Xenon 0.95/ 25 mm C-Mount Lens (Jos. Schneider Optische Werke GmbH, Bad Kreuznach, Germany) was also utilized. It covered a 1" format sensor with a 16 mm image circle. The high aperture (f/0.95) provided good image quality even under low light conditions. Xenon lenses were designed to cover the visible spectrum (400-700 nm). Therefore, the overall spectral sensitivity of the camera and lens system was reduced to the visible region. Specifically for the imaging of two-hands simultaneously, the camera was placed 65 cm above the hands to achieve an adequate field of view encompassing both left and right hands.

The acquisition parameters for imaging two-hand human UPE were determined by recording a representative set of subjects with a range of acquisition settings. There is always a tradeoff between imaging time and resolution when choosing acquisition parameters. In situation of spontaneous UPE imaging this was especially

Image A

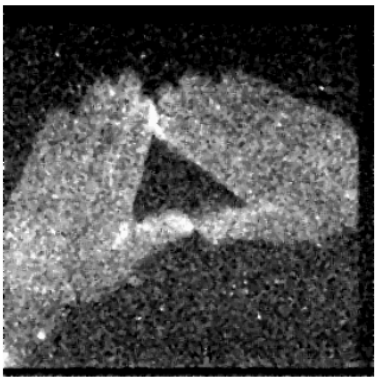

Image B

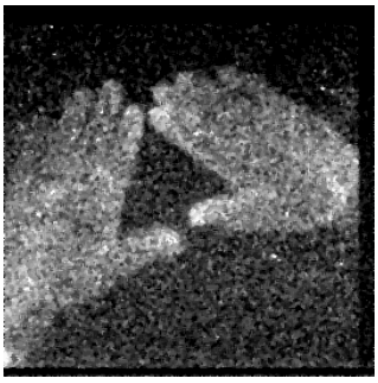

Image C

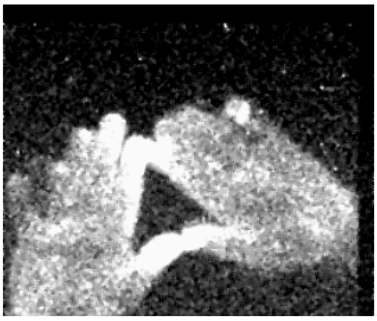

Image D

Figure 3. A series of images of the ultra-weak photon emission of palm hand sides of a single subject. Images were captured throughout two consecutive days. Image A: Day 1, early morning; Image B: Day 1, late afternoon; Image C: Day 2, early morning; Image D: Day 2, late afternoon.

important. The amount of time that subjects can sit still should be seriously considered. In the hand-imaging experiments the following settings were used: exposure time 1800 sec; binning 4 x 4; vertical shift speed 1.7 µsec; pixel readout rate 1 MHz; clock amplitude: normal; electron multiplying setting; EM gain level 300; pre-amplifier gain 5.2. Shorter exposure times did not give a sufficient signal. This could not be adequately compensated with a larger binning (e.g. 8 x 8) because cosmic ray effects and other noise could simultaneously affect a larger area of the image. The read out rate was the slowest possible to introduce the least noise.

A series of images of a single female subject was captured throughout the year. Each experimental day, the subject was imaged twice. The time between those two imaging periods was variable ranging between a few minutes and as long as 6 hours. No special measurement protocol was followed because in this preliminary state of the study, data on the variation in hand emission were not available. The series of images consisted of 11 sets (made on 11 different days). Each set included two images of the left and right dorsal sides of each hand. The first imaging each day provided a baseline image used for comparison with a second image made later on that same day. The first (baseline) images are presented in Figure 5. The Figure shows the high variability of emission intensity and pattern. In order to initiate a systematic evaluation and description of the

Image A

Image B

Image C

Image D

Image C: Day 2, early morning; Image D: Day 2, late afternoon.

images, we decided to distinguish three categories of images based on overall photon emission intensity. Category 1 includes the four images with the lowest emission intensity. Category 3 includes three images with the highest photon emission intensity and category 2 includes four images with intermediate overall intensity. In comparing the left and right hands, a high degree of similarity was observed. In those situations where a right hand emitted in a weak intensity manner, so did the left hand. The same was observed for the hand pairs with the intermediate and high emissions. However, the left-right symmetry was not perfect. An example of such difference in category 1 is B. In category 2, intensity differences or particular bright unilateral spots/areas are observed in E. The most intense images (category 3) included the greatest differences in emission pattern.

By zooming in on the specific features of the images with the weakest overall intensity, it was possible to document a pattern. In general, one or more finger end points emitted more light than the rest of the hand. In addition, a higher emission was detected on the medial side and the nail of the thumb plus, in some cases (i.e. image B), the lateral side of the index finger.

The images with moderate intensity documented that the category 1 spots with high intensity had become brighter and spread over a larger area of the fingers. Particularly, the medial side of the

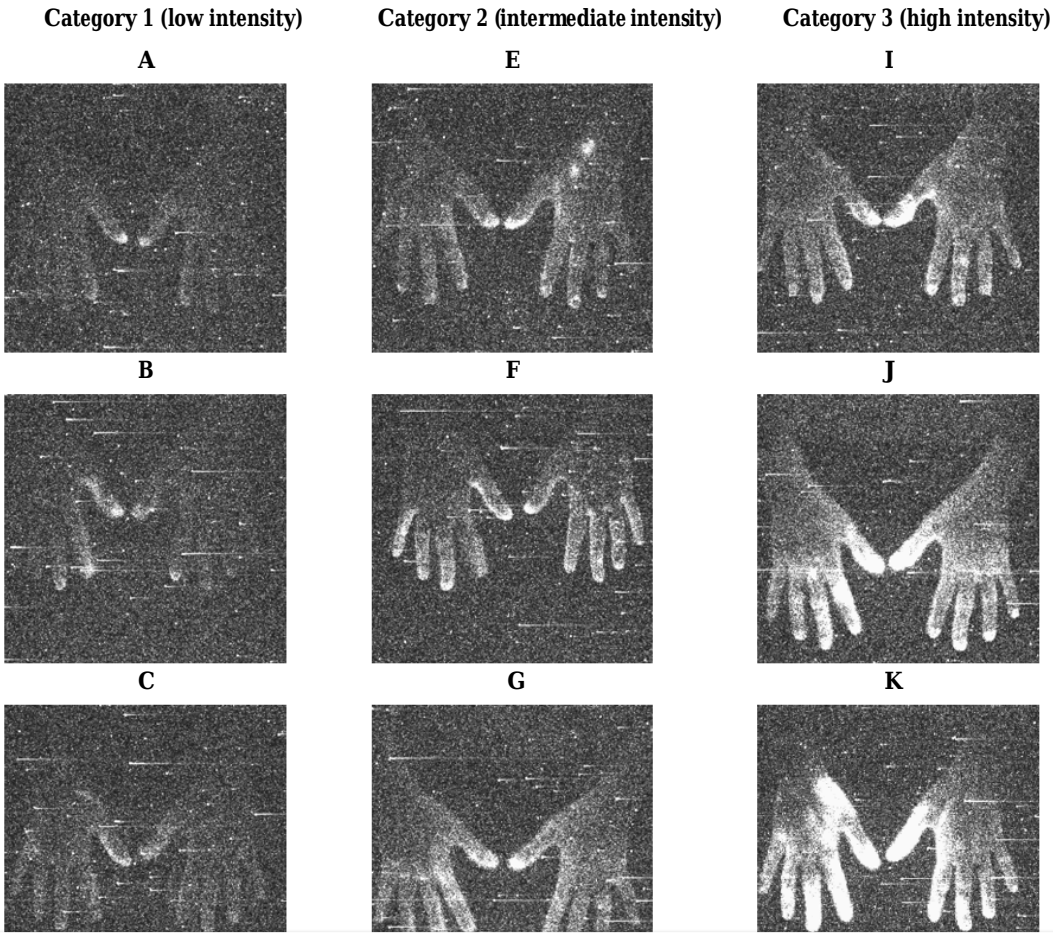

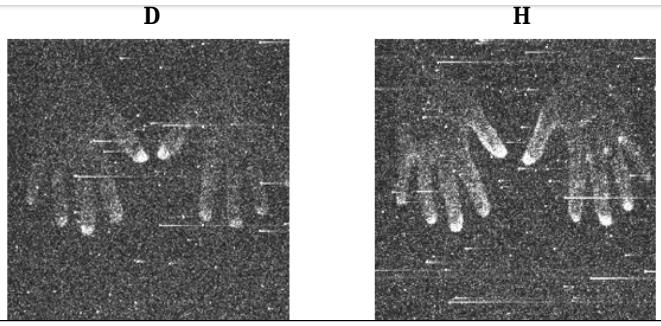

Figure 5. The variability in ultra-weak photon emission of the dorsal sides of the right and left hand of a single subject. In this collection of CCD images each image was the first of a pair made on the same experimental day. The images are categorized by intensity. Category 1 represents four images with lowest emission intensity. Category 3 represents three images with highest photon emission intensity and category 2 represents four images with intermediate overall intensity.

thumb including the finger tip emitted a relatively high intensity. At a higher overall intensity, more high-emission areas were detected as, for example, on the little finger (image F). Another interesting observation was the bright spot area on image E.

In the images with the highest overall intensity (category 3), in general, the hand areas with high intensity basically corresponded with category 2 but spread more in the direction of the central part of the hand. Most pronounced in intensity were the thumb and index fingers, plus other fingers that began to become more pronounced (i.e., image K). Apparently, a higher emission spread over a larger area as if the bright intensity (on the thumb side for instance) moved upwards on the radial side towards the wrist. This was more clearly illustrated on the right hand rather than on the left.

The most remarkable suggestion obtained from the images was that (except for some highly local bright spots on the back of the hand) the intensity spread from the end of one or more fingers in category 1 via the fingers in category 2 to the dorsal central area of the hand in category 3.

In order to test such spreading of intensity in time, the focus has been placed on the dynamics of the emission pattern. As explained before, two images were made on the same experimental day with the intermediate period being variable, ranging from a few minutes to up to 6 hours. If images were repeatedly measured within 2 hours both the intensity and pattern of emission remained the right hands were compared, it became evident that a high degree of similarity was present. However, the left-right symmetry was not perfect. Some differences in the emission patterns could be observed in the different intensity categories. Even in the images with the weakest overall intensity, it was possible to discover a pattern.

In general, one or more finger end points emitted more light than the rest of the hand. Images with moderate (category 2) intensity illustrated that the spots with high intensity in category 1 became brighter and spread over a larger area of the fingers. Hand areas with high intensity corresponded basically with the moderate images. However, there was spreading of photon emission in the direction of the central part of the hand. Most pronounced in intensity were the thumb and index fingers while simultaneously other fingers became more pronounced. Apparently, the higher emission covered a larger area as if the bright intensity (on the thumb side for instance) moved upwards on the radial side towards the wrist. This was more clearly illustrated on the right hand. If images were repeatedly measured within 2 hours, both the intensity and pattern of emission remained the same. When the intermediate time was more than 2 hours, additional dynamics could be observed.

DISCUSSION

This paper presents an unique line of research in the area of human ultra-weak photon emission imaging and its latest progress concerning the finding of patterns and their dynamics. Previous

the intermediate time is more than ... temporal dynamics could be observed. Two interesting examples are highlighted in Figure 6.

Image H illustrates a particular aspect of the pattern. No change was observed in overall intensity. However, the pattern of brightness of the individual finger tips of the left hand (right in the picture) had changed. Image K illustrates a decrease in overall photon emission intensity. A remarkable feature is the decrease in emission from the thumb up to the wrist, especially from the right hand (left in the picture). This pattern has remained the same although with less intensity.

In conclusion, there was a high variability in emission intensity and pattern. When left and

research [20-24] demonstrated that the body cannot be considered as a large, homogeneous emitter. Instead, emission is highly heterogeneous with high emitter anatomical locations such as the face and the hands. In the low emitting trunk and back parts of the body, no detailed light emission patterns were observed. In contrast, patterns with more details were detected in the high emitting face and hand regions. The detailed heterogeneity of the face shows higher emission around the mouth and the cheeks. Whereas, lower emission is found at the lateral area and the orbits [24]. The detailed heterogeneity of the hand emission is primarily illustrated by the major emission at finger tips [21, 22]. In the present results, the hands showed that the emission pattern is highly dynamic. Under conditions of increased emission,

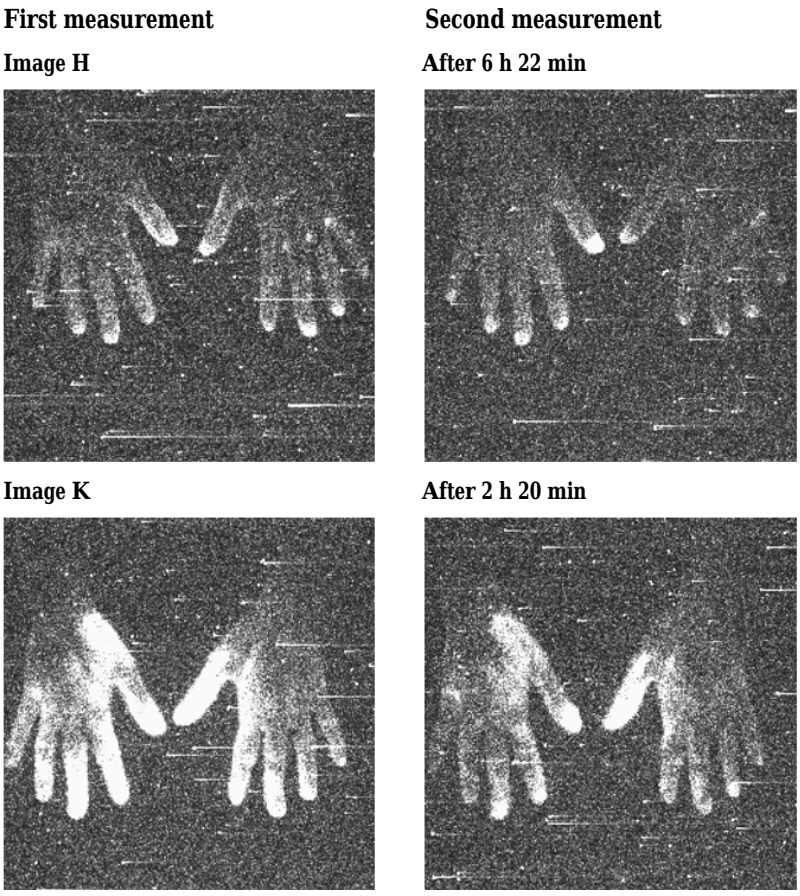

Figure 6. Illustrative examples of changes in ultra-weak photon emission of the dorsal sides of the right and left hand of a single subject. Each pair of images (first and second measurement) was made at the same day. The intermediate time interval is given in the figure. The coding of the images (H and K respectively) corresponds with the coding used in Figure 5.

localized at tips of thumb and index fingers, an increasing intensity continues over that particular site of the back of the hand. Another observation that we like to mention are the remarkable bright spots that are sometimes observed. These spots may correspond with acupuncture points according to the thinking of Inaba and colleagues [12] who focused attention on ultra-weak photon emission from hand and finger acupuncture points. They documented that emission intensity of acupuncture points was, in general, higher than

induced intensity enhancement of photon emission from other acupuncture points.

Following this line of thinking, the presented intensity patterns may be seen as part of the cutaneous zones which are related to specific "Channels". The "Channels" are an important and unique concept in traditional Chinese medicine [29-31]. They are regarded as passageways of Qi. Qi (also chi or ch'i) is an active principle in any living system. It is frequently translated as "life energy", "life force", or "energy flow".

According to the theory of Chinese medicine, twelve primary channels over the body can be distinguished. These channels not only reach into the body cavities to join with associated viscera, but also circulate through superficial connective tissues (muscles, tendon, ligaments) and on the surface of the body in defined cutaneous areas. Each of the broad surfaces of the cutaneous regions is superficially juxtaposed over the related channels.

With regard to the presented hand images in Figures 5 and 6, we will focus on the six hand channels, which are bilaterally oriented in the hand. They are divided in three yang channels in which the Qi is supposed to travel from the fingertips to the head, and another three yin channels in which the Qi travels from the internal organs to the finger tips. Their anatomical route, using the fingers as starting or end point is reflected in its name that include the organ associated with that particular channel. Thus, in the thumb, ends the "Arm Greater Yin Lung Channel". It descends along the upper arm and elbow to the pulse, and extends to the tip of the thumb. A branch from the main channel splits at the wrist, and travels to the tip of the index finger. The "Arm Yang Brightness Large Intestine Channel" begins at the tip of the index finger and proceeds upward to the wrist and upper arm. The "Arm Absolute Yin Pericardium Channel" descends along the arm, enters the palm and ultimately reaches the tip of the middle finger. A branch of this "Pericardium Channel" separates in the palm and proceeds along the 4th finger to the tip. Another channel, the "Arm Lesser Yang Triple Burner Channel" originates on the 4th fingertip, traversing the hand. The "Arm Greater

functions into a unified organism. Pathological symptoms associated with the primary channels are supposed to appear as local manifestations in their related cutaneous regions [29-31]. One step to proceed would be imaging the hands of different subjects to detect personalized patterns as well as the possibility to subtype subjects based on the principles of Chinese medicine. In this line of thinking, a further characterization of the cutaneous representation of the channels by using UPE measurements could lead to the introduction of a more personalized diagnostics and medicine.

ACKNOWLEDGEMENTS

We thank Prof. Masaki Kobayashi for many years of collaboration. He and his students offered at many occasions his specialized CCD equipment for obtaining human and animal ultra-weak photon emission images. We appreciate his broad technical and theoretical knowledge.

The authors also thank Everine B. van de Kraats, PhD, for providing the CCD system set up description under 'Further progress in emission dynamics: the focus on dorsal of hands' and the raw preliminary images (Figure 6 and 7) that she acquired while developing the CCD imaging protocol. The images are displayed with a window leveling of 200-1200 and are not flat-field corrected. The protocol considerations will be described in Van de Kraats, E. B. Guidelines and technical notes for spontaneous ultra-weak photon emission of human hands with EMCCD camera (in progress). The authors thank Dr. John Ackerman for his assistance in editing the text.

REFERENCES

1. Dobrin, R., Kirsch, C., Kirsch, S., Pierrakos, J., Schwartz, E., Wolff, T. and Zeira, Y.

Channel" descends along the arm, enters the palm and proceeds to the finger tip of the little finger.

In principle, it is possible that the distribution of Qi over the specific channels is related to specific dynamic emission patterns. This hypothesis, of course, needs more systematic study.

According to traditional theory, the channels integrate all the body's separate parts and

1979, Pychoenergetic Systems: The Interface of Consciousness, Energy and Matter: Experimental measurements of the human energy field, S. Krippner (Ed.), Gordon and Breach, New York, 227.
2. Tsuchiya, Y., Inuzuka, E., Kurono, T. and Hosoda, M. 1985, J. Imag. Technol., 11, 1084-1088.
3. Mashiko, S., Kobayashi, M., Saeki, R., Hishinuma, K., Yoda, B., Ichinura, T. and Inaba, H. 1987, Photomed. Photobiol., 9, 101-102.

4. Usa, M., Scott, R. Q., Kobayashi, M., Nagoshi, T., Watanabe, N. and Inaba, H. 1988, Photomed. Photobiol., 10, 55-68.
5. Scott, R. Q., Usa, M. and Inaba, H. 1989, Appl. Phys. B., 48, 183-185.
6. Scott, R. Q. and Inaba, H. 1989, J. Biolum. Chemilum., 4, 507-511.
7. Inaba, H., Scott, R. Q., Usa, M., Kobayashi, M. and Ichimura, T. 1990, Laser/ Optoelectronics in Medicine, W. Waidelich, and R. Waidelich (Eds.), Springer-Verlag, Berlin, 313-316.
8. Suzuki, S., Usa, M., Nagoshi, T., Kobayashi, M., Watanabe, N., Watanabe, H. and Inaba, H. 1991, J. Photochem. Photobiol. B, 9, 211-217.
9. Usa, M., Devaraj, B., Kobayashi, M., Takeda, M. and Inaba, H. 1993, Digest of Technical Papers, The 7th International Conference on Solid-State Sensors and Actuators, June 7-10, Yokohama, Japan, 1058-1061.
10. Devaraj, B., Ito, H., Roschger, P., Scott, R. Q., Usa, M., Kobayashi, M., Taguchi, Y. and Inaba, H. 1991, Proceedings of the conference on Emerging Optoelectronic Technologies. A. Selvarajan, B. S. Sonde, K. Shenai, V. K. Tripathi (Eds.), Bangalore, India, December 16-20, 192-196.
11. Usa, M., Devaraj, B., Kobayashi, M., Takeda, M., Ito, H., Jin, M. and Inaba, H. 1994, Optical methods in biomedical and environmental sciences, H. Ohzu, and S. Komatsu (Eds.) Elsevier Sciences, Amsterdam, 3.
12. Inaba, H. 2000, Journ. of Internat. Soc. Life Inform. Sci., 18, 448-456.
13. Usa, M., Kobayashi, M., Suzuki, S., Ito, H. and Inaba, H. 1991, ITEJ Technical Report, 15.
17. Kobayashi, M., Devaraj, B., Usa, M., Tanno, Y., Takeda, M. and Inaba, H. 1997, Photochem. Photobiol., 65, 535-537.
18. Kobayashi, M., Takeda, M., Ito, K. I., Kato, H. and Inaba, H. 1999, J. Neurosci. Methods, 93, 163-168.
19. Kobayashi, M., Takeda, M., Sato, T., Yamazaki, Y., Kaneko, K., Ito, K. I., Kato, H. and Inaba, H. 1999, Neurosci. Res., 93, 103-113.
20. Kobayashi, M. 2003, Energy and Information Transfer in Biological Systems. F. Musumeci, L. S. Brizhik and M. W. Ho (Eds.), World Scientific Publishing, New Jersey, London, 157-187.
21. Kobayashi, M. 2005, Biophotonics - Optical Science and Engineering for the 21st Century. X. Shen and R. Van Wijk (Eds.), Springer, New York, 155-170.
22. Van Wijk, R., Kobayashi, M. and Van Wijk, E. P. A. 2006, J. Photochem. Photobiol. B., 83, 69-76.
23. Van Wijk, E. P. A., Kobayashi, M. and Van Wijk, R. 2006, Biophotons and Coherent Systems in Biology, Biophysics and Biotechnology, L. Beloussov, V. L. Voeikov, and V. S. Martynyuk (Eds.), Kluwer, New York, 177-189.
24. Kobayashi, M., Kikushi, D. and Okamura, H. 2009, PLoS ONE, 4, 6256.
25. Van Wijk, E. P. A., Lüdtke, R. and Van Wijk, R. 2008, J. Altern. Complement. Med., 14, 241-50.
26. Van Wijk, E. P. A., Van Wijk, R. and Bajpai, R. 2008, Indian J. Exp. Biol., 46, 345-352.
27. Inaba, H. 1998, Proceedings of the Institute of Electrostatics, 22, 245-252.
28. Inaba, H. 1999, Opt. Electro-opt. Eng. Contact, 37, 251-267.

Usa, M. and Inaba, H. 1995, Urological Res., 23, 315-318.
16. Kobayashi, M., Devaraj, B., Usa, M., Tanno, Y., Takeda, M. and Inaba, H. 1996, Frontiers Med. Biol. Eng., 7, 299-309.
29. Agren, H. 1975, Medicine in Chinese Cultures. A. Kleinman (Ed), NIH, Washington, 37-60.
30. Kaptchuk, T. 1983, The Web that has no Weaver: Understanding Chinese Medicine. Congdon & Weed, New York.
31. Porkert, M. 1974, The Theoretical Foundations of Chinese Medicine, The MIT Press, Cambridge, Massachusetts.